Adarraga I, Romera J, Cantera M, Insausti N, Mujika F. *Application of the dual integrated force method to the analysis of the off-axis three-point flexure test of unidirectional composites*. **Journal of Composite Materials**. 2016;50(3):413-426. Copyright © The Author(s) 2015, published by Sage https://doi.org/10.1177/0021998315576377

APPLICATION OF THE DUAL INTEGRATED FORCE METHOD TO THE ANALYSIS OF THE OFF-AXIS THREE-POINT FLEXURE TEST OF UNIDIRECTIONAL COMPOSITES

I. Adarraga, J. M. Romera, M. A. Cantera, N. Insausti, F. Mujika
Materials + Technologies Group. Department of Mechanical Engineering. Polytechnic University College. University of the Basque Country (UPV/EHU).
Plaza Europa, 1, 20018 San Sebastián, Spain.
E-mail: itziar.adarraga@ehu.es

ABSTRACT

This paper shows the use of the Dual Integrated Force Method in the Finite Element Method and its application to unidirectional composite laminates. This method was developed by S.N. Patnaik for isotropic materials, considering not only the equilibrium equations but also the compatibility conditions. The method is applied to obtain the stiffness matrix of a four node rectangular plate element. Then, a three-point flexure test of a unidirectional off-axis composite has been analyzed. The results obtained with this method have been compared with those obtained from a previous analytic approach and with those obtained by commercial software of Finite Element Method, which is based on the Stiffness Method.

Keywords: Dual Integrated Force Method, Stiffness method; Theorems of virtual work; laminate composites.

---

1. INTRODUCTION

Usually, the Stiffness Method (SM) is used in the numerical analysis of composite materials. In spite that Hoa [1] published a book dealing with the application of Hybrid Method (HM) for stress analysis of laminated composites, it seems that these methods have been barely used in last years in the analysis of composites. Otherwise, it has been recently shown that the Dual Integrated Force Method (IFMD) developed by Patnaik and the HM developed by Pian are equivalent [2]. In the present work, a linear elastic analysis of an off-axis three-point flexure test which has been previously analyzed analytically, experimentally and numerically is carried out after formulating a plate element in IFMD, as an alternative to SM.

In the three-point flexure test of unidirectional off-axis composites, bending-twisting coupling can cause the lift-off of the specimen on the fixture supports. When lift-off occurs, contact between specimen and fixture support is located at two opposite corners as shown in Figure 1, and twisting moments appear. Some works have dealt with the three-point flexure test of unidirectional off-axis composites. Mujika et al. [3] proposed an analytical method for determining in-plane shear modulus by three-point flexure of unidirectional composites oriented at 45º. In later works, the conditions for lift-off of the specimen were determined and the displacement field of an off-axis composite in three-point flexure was determined [4]. Lift-off and no lift-off situations were considered and the approach was extended to the calculation of the displacement field for any fiber orientation. Five fibre orientations and ten different spans for each orientation were used for comparing analytic and experimental results of a carbon- epoxy composite. Results concerning the displacement of the load application point were compared, obtaining good agreement [5]. In a recent work, the analytical approach has been extended to multidirectional laminates [6].

The displacement and stress field of unidirectional off-axis composites in three-point flexure has been also analysed by FEM [7]. In this work a linear elastic analysis has been carried out, using shell and solid elements based on the SM. The SM is a displacement based formulation directly derived from the Principle of Virtual Work (PVW), assuming a compatible displacement field. The application of the PVW ensures the fulfilment of equilibrium equations as a function of the nodal displacements. On the other hand, Force method (FM) [8] is based on the assumption of an equilibrated stress field. The force variables are the principal unknowns and are separated into static and redundant forces. The application of the Principle of Complementary Virtual Work (PCVW) ensures that the compatibility equations are satisfied, assuming an equilibrated stress field [9].

The Integrated Force Method (IFM) was developed in 1973 by Patnaik et al. [10,11] for discrete structures. In this method it appears the idea of using not only the equilibrium equations, but also the compatibility conditions. The application of the PCVW ensures that compatibility equations are satisfied as a function of the assumed stress parameters. In later works, IFM was applied to continuous systems [12,13] and was compared with the FM and SM [14-16]. In the finite element method, the stresses and displacements [17] obtained by IFM converge to the correct solution faster than the same solution generated by the SM. In 1998, Patnaik et al. [18] developed a dual form for the IFM which provides identical solutions for stresses and displacements, named IFMD. It was based on the same formulation that the IFM, but the structure of the governing equation is similar to SM. IFMD has two set of equations: one for the calculation of displacements, and other for the calculation of forces or stresses [19]. The SM has one set of equations to calculate displacements, and stresses are calculated by differentiating the displacements to determine strains, and then transforming strains in stresses by the Hooke's law. Otherwise, the HM is based on the Hellinger-Reissner variational principle [20,21], assuming independent stress and displacement fields. As stated before, IFMD and HM are equivalent.

A disadvantage of IFMD and HM is the additional computational cost of the inversion of the flexibility matrix required to construct the stiffness matrix. This disadvantage has been solved by Zhang et al. [22,23] by means of the diagonalization of the flexibility matrix.

Recently, new applications of IFM to FE analysis have been published [24-29]. These works deal with the development of the new elements for thick and moderately thick isotropic plates, and the generation of equilibrium and flexibility matrix for plate elements.

The aim of this manuscript is to formulate a plate element by IFMD, without considering out-of-plane shear effects. This element is valid for symmetric laminates where membrane-plate coupling is not present, when shear effects are negligible. In particular, it is used for analysing the three-point flexure test of a unidirectional composite. As pointed out above, there are previous analytic, experimental and numeric results concerning this problem that have been used as reference. Moreover, results obtained by IFMD have been compared also with those provided by ABAQUS with the same number of shell elements.

2. DUAL INTEGRATED FORCE METHOD

2.1. Governing Equation

In the present section the elemental formulation of IFMD has been obtained from the direct application of the PVW and PCVW. Its governing equation is similar to the equations of SM as the displacements are the primary unknowns.

It is assumed that a continuum has been discretized in finite elements. Assuming that each element has n degrees of freedom in displacements, the PVW [9,30] states that,

$$\int_V \{\delta\varepsilon\}^T \{\sigma\} dV = \{\delta a^i\}^T \{P^i\} \tag{1}$$

Where $i = 1$ to n; V is the volume of the element; $\{\delta a^i\}$ is the vector of virtual nodal displacements; $\{P^i\}$ is the vector of nodal external forces; $\{\delta\varepsilon\}$ is the vector of virtual strains; and $\{\sigma\}$ is the vector of stress components.

Otherwise, the PCVW [9,30] states that:

$$\int_V \{\delta\sigma\}^T \{\varepsilon\} dV = \{\delta P^i\}^T \{a^i\} \tag{2}$$

In the same manner than in SM, the displacements at any point of the element are related to the nodal displacements by means of interpolation functions [31,32]. From the displacements, strains at any point of the element are:

$$\{\varepsilon\} = [L][N]\{a^i\} = [B]\{a^i\} \tag{3}$$

Where $[B]$ is the nodal displacement-strain matrix; $[N]$ is the matrix of displacement interpolation functions; and $[L]$ is the matrix of the differential operators, the same matrices than in SM. Furthermore, stresses and strains are related by the flexibility matrix of the material $[S]$, being:

$$\{\varepsilon\} = [S]\{\sigma\} \tag{4}$$

In SM the stresses are obtained from the strains and displacements. However, in IFMD the stress field is approximated by using polynomials of the appropriate order [33-35]**.** The independent internal forces in a finite element are a set of independent forces that satisfy equilibrium equations and, by means of force interpolation functions, reproduce the stress field of the element. Assuming that each element has m degrees of freedom of forces, stresses at any point of the element are expressed as:

$$\{\sigma\} = [Y]\{F^j\} \tag{5}$$

Where $j = 1$ to m. Then, replacing equations (3) and (5) in equation (1), the equilibrium equation is obtained:

$$\begin{gathered} \left(\int_V [B]^T [Y] dV\right)\{F^j\} = \{P^i\} \\ [E^e]\{F^j\} = \{P^i\} \end{gathered} \tag{6}$$

Being $[E^e] = \int_V [B]^T [Y] dV$ the equilibrium matrix of the element. This matrix has dimensions (n x m), being n and m the degrees of freedom of displacements and forces of the element, respectively. It is equivalent to the leverage matrix of HM. In HM Leverage matrix is obtained form the Hellinger-Reissner variational principle, putting it in terms of nodal displacements and internal forces by means of interpolation functions. This way of calculation does not show that this matrix relates the internal forces with external forces, relation shown in Equilibrium equation (6) [2,20].

By replacing equations (4), (5) and (6) into the equation (2) it results:

$$\left(\int_V [Y]^T [S][Y] dV\right)\{F^j\} = \left[E^e\right]^T \{a^i\}$$
$$\left[G^e\right]\{F^j\} = \left[E^e\right]^T \{a^i\} \tag{7}$$

Being $\left[G^e\right] = \int_V [Y]^T [S][Y] dV$ the flexibility matrix of the element [8]. Extracting $\{F^j\}$ from (7):

$$\{F^j\} = \left[G^e\right]^{-1} \left[E^e\right]^T \{a^i\} \tag{8}$$

Multiplying by $[E^e]$ the two members of Equation (8) and replacing Equation (6):

$$\left(\left[E^e\right]\left[G^e\right]^{-1}\left[E^e\right]^T\right)\{a^i\} = \{P^i\}$$
$$\left[K^e\right]\{a^i\} = \{P^i\} \tag{9}$$

Where $\left[K^e\right] = \left[E^e\right]\left[G^e\right]^{-1}\left[E^e\right]^T$ is the stiffness matrix of the element corresponding to IFMD. The stiffness matrix of the system is obtained following standard assembly procedures. Thus, the governing equation of IFMD is:

$$[K]\{a^l\} = \{P^l\} \tag{10}$$

Where $l = 1$ to N, being N the degrees of freedom in displacements of the analyzed model. From Equation (10) the nodal displacements of the structure are determined. The internal forces of each element are obtained from Equation (8) and the stresses at any point of the element from Equation (5). Finally, the strains are obtained by the constitutive relation given in Equation (4).

The drawback of IFMD is the great computational cost associated with the inversion of the flexibility matrix. Indeed, the difference in computational cost with respect to SM is located in the element formulation for the same number of elements, as the assembly of the total stiffness matrix and the solution of the equation system is similar in both cases. This aspect can be improved by the diagonalization of this matrix proposed by Zhang [22,23].

2.2. Formulation of a plate element

The four node rectangular plate-bending element of Figure 2 is used for implementing IFMD. In the case of bending, the components of the strain field along the thickness are [15]:

$$\{\varepsilon\} = z\{\kappa\} = z\left[B_P\right]\{a^i\} = z\begin{Bmatrix} -\dfrac{\partial^2 [N]}{\partial x^2} \\ -\dfrac{\partial^2 [N]}{\partial y^2} \\ -\dfrac{\partial^2 [N]}{\partial x \partial y} \end{Bmatrix}\{a^i\} \tag{11}$$

Where $\{\kappa\}$ are bending and twisting curvatures, which are obtaining by:

$$\{\kappa\} = [d]\{M\} \tag{12}$$

Where $\{M\}$ is the vector of resultant moments, and [d] the compliance matrix of the material given by [36]:

$$[d]=\begin{bmatrix} d_{xx} & d_{xy} & d_{xs} \\ d_{yx} & d_{yy} & d_{ys} \\ d_{sx} & d_{sy} & d_{ss} \end{bmatrix} \tag{13}$$

[B_p] is the nodal displacement-strain matrix and it is obtained by differentiation of the displacement interpolation functions. The shape functions for this element are formed combining the same third order Hermite polynomials than in SM in the case of the beam element with two nodes [31,32]:

$$\begin{aligned} N_1(\xi) &= \tfrac{1}{4}\left(2-3\xi+\xi^3\right) \\ \bar{N}_1(\xi) &= \tfrac{a}{4}\left(1-\xi-\xi^2+\xi^3\right) \\ N_2(\xi) &= \tfrac{1}{4}\left(2+3\xi-\xi^3\right) \\ \bar{N}_2(\xi) &= \tfrac{a}{4}\left(-1-\xi+\xi^2+\xi^3\right) \end{aligned} \tag{14}$$

Where $\xi = x/a$ and $\eta = y/b$ are natural coordinates. The polynomial displacement function is:

$$\begin{aligned} w &= N_1(\xi)N_1(\eta)w_1 + \bar{N}_1(\xi)N_1(\eta)\theta_{x1} + N_1(\xi)\bar{N}_1(\eta)\theta_{y1} + N_2(\xi)N_1(\eta)w_2 + \\ &+ \bar{N}_2(\xi)N_1(\eta)\theta_{x2} + N_2(\xi)\bar{N}_1(\eta)\theta_{y2} + N_2(\xi)N_2(\eta)w_3 + \bar{N}_2(\xi)N_2(\eta)\theta_{x3} + \\ &+ N_2(\xi)\bar{N}_2(\eta)\theta_{y3} + N_1(\xi)N_2(\eta)w_4 + \bar{N}_1(\xi)N_2(\eta)\theta_{x4} + N_1(\xi)\bar{N}_2(\eta)\theta_{y4} \end{aligned} \tag{15}$$

Where $w_i, \theta_{xi}, \theta_{yi}$, are the twelve displacement degrees of freedom of the element, corresponding to a displacement and two rotations per node. The polynomial of Equation (15) has been obtained by eliminating the twist-terms from the fourth order complete polynomial [31]. That polynomial ensures the continuity of displacements between rectangular elements. The function of Equation (15) is the same used by Patnaik in the formulation of a plate element in IFMD [19]. By substituting Equation (11), the PVW becomes,

$$\int_V z\left\{\delta a^i\right\}^T\left[B_p\right]^T\{\sigma\}dV=\left\{\delta a^i\right\}^T\left\{P^i\right\} \tag{16}$$

And thus,

$$\left\{\delta a^i\right\}^T\int_S \{M\}\left[B_p\right]dS=\left\{\delta a^i\right\}^T\left\{P^i\right\} \tag{17}$$

Where S is the surface of the plate and $\{M\}$ the vector of resultant moments given by:

$$\{M\}=\int_t z\{\sigma\}^T dz \tag{18}$$

Where t indicates the thickness. In the case of a plate, Equation (5) becomes in:

$$\{M\}=[Y]\left\{F^j\right\} \tag{19}$$

Being the parameters $\left\{F^j\right\}$ in Equation (19) moments per unit length. Then, replacing Equation (19) in (17), as $\{\delta a^i\}^T$ are independent, the equilibrium equation is:

$$\left[E^e\right]\left\{F^j\right\}=\left\{P^i\right\} \tag{20}$$

When $[E^e]$ is the equilibrium matrix of a plate element, being:

$$\left[E^e\right]=\int_S\left[B_p\right]^T\left[Y\right]dS \tag{21}$$

For a rectangular plate, according to Equation (19), the selected force interpolation functions have been derived from the stress functions, based on third order Hermite polynomials [33,35] with nine independent parameters, being:

$$\begin{aligned} M_x &= F_1+F_2\eta+F_3\xi+F_4\eta\xi \\ M_y &= F_5+F_6\eta+F_7\xi+F_8\eta\xi \\ M_{xy} &= F_9 \end{aligned} \tag{22}$$

As in the case of interpolation functions of displacements, natural coordinates are used, being $\xi = x/a$ and $\eta = y/b$. According to Equations (19) and (22), the matrix of the interpolation functions is:

$$\boldsymbol{Y}=\begin{bmatrix} 1 & \eta & \xi & \eta\xi & 0 & 0 & 0 & 0 & 0 \\ 0 & 0 & 0 & 0 & 1 & \eta & \xi & \eta\xi & 0 \\ 0 & 0 & 0 & 0 & 0 & 0 & 0 & 0 & 1 \end{bmatrix} \tag{23}$$

Replacing $[B_p]$ from Equation (11) and $[Y]$ from Equation (23) in Equation (21) the equilibrium matrix of the element is

$$\left[E^e\right]=\begin{pmatrix} 0 & -b & 0 & \frac{2}{5}b^2 & 0 & 0 & -a & \frac{2}{5}a^2 & -2 \\ 0 & \frac{-1}{3}b^2 & 0 & \frac{1}{15}b^2 & a & \frac{-2}{5}a^2 & ab & \frac{2}{5}a^2b & 0 \\ b & -ab & \frac{-1}{5}b^2 & \frac{2}{5}ab^2 & 0 & 0 & \frac{-1}{3}a^2 & \frac{1}{15}a^2 & 0 \\ 0 & b & 0 & \frac{-2}{5}b^2 & 0 & 0 & -a & \frac{-2}{5}a^2 & 2 \\ 0 & \frac{1}{3}b^2 & 0 & \frac{-1}{15}b^2 & a & \frac{2}{5}a^2 & -ab & \frac{-2}{5}a^2b & 0 \\ -b & -ab & \frac{1}{5}b^2 & \frac{2}{5}ab^2 & 0 & 0 & \frac{1}{3}a^2 & \frac{1}{15}a & 0 \\ 0 & b & 0 & \frac{2}{5}b^2 & 0 & 0 & a & \frac{2}{5}a^2 & -2 \\ 0 & \frac{-1}{3}b^2 & 0 & \frac{-1}{15}b^2 & -a & \frac{-2}{5}a^2 & -ab & \frac{-2}{5}a^2b & 0 \\ -b & -ab & \frac{-1}{5}b^2 & \frac{-2}{5}ab^2 & 0 & 0 & \frac{-1}{3}a^2 & \frac{-1}{15}a & 0 \\ 0 & -b & 0 & \frac{-2}{5}b^2 & 0 & 0 & a & \frac{-2}{5}a^2 & 2 \\ 0 & \frac{-1}{3}b^2 & 0 & \frac{1}{15}b^2 & -a & \frac{2}{5}a^2 & ab & \frac{2}{5}a^2b & 0 \\ b & -ab & \frac{1}{5}b^2 & \frac{-2}{5}ab^2 & 0 & 0 & \frac{1}{3}a^2 & \frac{-1}{15}a & 0 \end{pmatrix} \tag{24}$$

According to Equations (11) and (12) the components of the strain field can be expressed as:

$$\{\varepsilon\}=z\left[d\right]\left\{M\right\} \tag{25}$$

Then, replacing Equation (25) in the PCVW of Equation (2):

$$\int_V z\{\delta\sigma\}^T [d]\{M\} dV = \{\delta P^i\}^T \{a^i\} \tag{26}$$

Taking into account Equation (18), Equation (26) can be expressed as

$$\int_S \{\delta M\}^T [d]\{M\} dS = \{\delta P^i\}^T \{a^i\} \tag{27}$$

Replacing Equations (19) and (20) in Equation (27),

$$\{\delta F^j\}^T [G^e]\{F^j\} = \{\delta F^j\}^T [E]^T \{a^i\} \tag{28}$$

Being $[G^e]$ the flexibility matrix of a plate element,

$$[G^e] = \int_S [Y]^T [d][Y] dS \tag{29}$$

Replacing $[Y]$ from Equation (23) and $[d]$ from Equation (13) in Equation (29) the flexibility matrix of the element is

$$[G^e] = 4ab \begin{bmatrix} d_{xx} & 0 & 0 & 0 & d_{xy} & 0 & 0 & 0 & d_{xs} \\ 0 & \frac{1}{3}a^2 d_{xx} & 0 & 0 & 0 & \frac{1}{3}a^2 d_{xy} & 0 & 0 & 0 \\ 0 & 0 & \frac{1}{3}b^2 d_{xx} & 0 & 0 & 0 & \frac{1}{3}b^2 d_{xy} & 0 & 0 \\ 0 & 0 & 0 & \frac{1}{9}a^2 b^2 d_{xx} & 0 & 0 & 0 & \frac{1}{9}a^2 b^2 d_{xy} & 0 \\ d_{xy} & 0 & 0 & 0 & d_{yy} & 0 & 0 & 0 & d_{ys} \\ 0 & \frac{1}{3}a^2 d_{xy} & 0 & 0 & 0 & \frac{1}{3}a^2 d_{yy} & 0 & 0 & 0 \\ 0 & 0 & \frac{1}{3}b^2 d_{xy} & 0 & 0 & 0 & \frac{1}{3}b^2 d_{yy} & 0 & 0 \\ 0 & 0 & 0 & \frac{1}{9}a^2 b^2 d_{xy} & 0 & 0 & 0 & \frac{1}{9}a^2 b^2 d_{yy} & 0 \\ d_{xs} & 0 & 0 & 0 & d_{ys} & 0 & 0 & 0 & d_{ss} \end{bmatrix} \tag{30}$$

Replacing the equilibrium matrix of Equation (24) and the flexibility matrix of Equation (30) in Equation (9) the stiffness matrix of the element is obtained. The stiffness matrix of the system is achieved by assembling the stiffness matrices of the elements, in the same manner than in SM. After obtaining the displacements, the determination of other unknowns is different for IFMD and SM. Both calculation processes are summarized in Table 1.

Table 1: Procedures to obtaining stresses in IFMD and SM

Steps for the formulation	***IFMD***	***SM***
Stiffness matrix	$[K]_{IFMD} \{a^l\} = \{P^l\}$	$[K]_{SM} \{a^l\} = \{P^l\}$
Displacements	$\{a^l\}$	$\{a^l\}$
Independent element forces	$\{F^j\} = [G^e]^{-1} [E^e]^T \{a^i\}$	
Resultant moments	$\{M\} = [Y]\{F^j\}$	
Plate curvatures	$\{\kappa\} = [d]\{M\}$	$\{\kappa\} = [B_p]\{a^i\}$
Strains	$\{\varepsilon\} = z\{\kappa\}$	
Stresses	$\{\sigma\} = [Q]\{\varepsilon\}$	

The stiffness matrix for a lamina of the symmetric laminate necessary for determining stresses is given by [36]:

$$[Q]=\begin{bmatrix} Q_{xx} & Q_{xy} & Q_{xs} \\ Q_{xy} & Q_{yy} & Q_{ys} \\ Q_{xs} & Q_{ys} & Q_{ss} \end{bmatrix}$$

3. ANALYTICAL MODEL

For obtaining the displacement field of an off-axis specimen in three-point flexure [6], it has been divided in four parts as shown in Figure 3. Displacement field was the same in A, D parts and in B, C parts due to symmetry with respect to the central point of the specimen, named central symmetry. Moreover, each part has a different reference system, as shown in Figure 3. Neglecting shear effects, the displacement field in A, D parts is given by:

$$w_{M1}(x_0,y_0)=\frac{PL^2}{96c^3}\left\{\begin{array}{l} 2d_{xx}\left(4x_0^3+3x_0\right)c^4+3d_{xs}\left(2kx_0+2x_0^2(1-k)+y_0-4x_0^2y_0\right)c^3+ \\ +\left[3hd_{ss}\left(x_0+y_0-2x_0y_0\right)+6d_{xy}g\left(-x_0^2+x_0-y_0^2+y_0\right)\right]c^2+ \\ +3d_{ys}g\left(2ky_0+2y_0^2(1-k)+x_0-4x_0y_0^2\right)c+2d_{yy}g\left(-4y_0^3+3y_0\right) \end{array}\right\} \tag{31}$$

$$0<x_0<\tfrac{1}{2} \qquad 0<y_0<\tfrac{1}{2}$$

Where w_{M1} is the displacement term due to bending-twisting in A, D parts. On the other hand, the displacements of any point in B, C parts was given by,

$$w_{M2}(x_0,y_0)=\frac{PL^2}{96c^3}\left\{\begin{array}{l} 2d_{xx}\left(3x_0-4x_0^3\right)c^4+3d_{xs}\left[1+2kx_0-y_0+2x_0^2(1+k)+4x_0^2y_0\right]c^3+ \\ +\left[3kd_{ss}\left(1-x_0-y_0+2x_0y_0\right)+6d_{xy}g\left(x_0+y_0-x_0^2-y_0^2\right)\right]c^2+ \\ +3d_{ys}g\left(1-x_0+2ky_0-2y_0^2(1+k)+4x_0y_0^2\right)c+2d_{yy}g\left(3y_0-4y_0^3\right) \end{array}\right\} \tag{32}$$

$$0<x_0<\tfrac{1}{2} \qquad 0<y_0<\tfrac{1}{2}$$

Where w_{M2} is the displacement term due to bending-twisting coupling in B, C parts. In Equations (31) and (32) P is the load; x and y are the Cartesian coordinates in the coordinate systems of A, B, C and D parts; $x_0 = x/L$ and $y_0 = y/L$ are normalized coordinates; L is the distance between the support cylinders (span); b is the specimen width; $c = L/b$ is the span-to-width ratio; h is the specimen thickness; L' is the specimen length, $g = L/L'$ is the span-to-overall-length ratio; θ is the fiber orientation angle; and k is the twisting ratio.

The twisting ratio k is the ratio between twisting moment when lift-off does not occur and when it does. When lift-off occurs k = 1, and when lift-off does not occurs, k<1 and the contact is assumed at the four corners.

In a unidirectional laminate, in-plane stress components in the case that lift-off occurs are given by:

$$\sigma_x=\frac{3P}{h^2}cx_0 \tag{33}$$

$$\sigma_y=\frac{3P}{h^2}\frac{g}{c}y_0 \tag{34}$$

$$\tau_{xy}=\tau_s=\frac{3P}{4h^2} \tag{35}$$

4. UNIDIRECTIONAL COMPOSITE IN OFF-AXIS THREE-POINT FLEXURE

4.1. Geometry and material properties

In a general multidirectional composite the plate behaviour is coupled with the membrane behaviour. In the case of a symmetric laminate, membrane-plate coupling does not exist. The formulation of a plate element takes into account the plate behaviour that basically includes the relation between bending and twisting curvatures and applied moments, as shown in Equation (12). In the case of membrane-plate coupling, shell elements would be necessary. Then, the element formulated is valid for the analysis of symmetric laminates under the action of moments. In particular, the unidirectional case is considered as there are previous analytic, experimental and numerical results [3-4,5,6,7].

A three-point flexure test for the unidirectional off-axis laminate shown in Figure 1 has been analyzed by IFMD with four, eight and sixteen elements, for obtaining the displacement and stress field. The elastic properties correspond to a carbon fiber/epoxy composite [3], being: E_L=142 GPa; E_T=8.9G Pa; ν_{LT}= 0.27; $\nu_{TT'}$= 0.3; G_{LT}=4.8 GPa; $G_{LT'}$=4.8 GPa; $G_{TT'}$=3.4 GPa.

4.2. Comparison with previous analytic and numeric results

The results of IFMD analysis have been compared with the numerical analysis realized by Romera et al. [7] with the commercial software COSMOS/M based on the SM. In this analysis, named Complete Model, 1960 shell elements based in Reissner - Mindlin theory have been utilized. The load and support rollers have been modelled as infinitely rigid cylinders. The contact between the rollers and the specimen is modelled with node-to-node linear gap elements. Thus, when lift-off occurs, the contact between the specimen and the support cylinders is reduced to two points. Both results have been compared with those obtained by the analytical approach developed by Mujika et al. [4,5], which has been described in the previous section. This approach was compared with experimental results, as it has been pointed out in the introduction.

Moreover, the results obtained from IFMD with sixteen elements have been compared with those obtained by the commercial software ABAQUS with the same number of general-purpose conventional shell elements S4R, that neglect shear effects in the case of thin plates. Except in the Complete Model, all other methods assume that the contact between the load roller and specimen occurs at a point.

The dimensions and the load are: L = 120 mm; b = 15 mm; h = 2.114 mm and P = 46 N. The fiber direction with respect to the longitudinal direction is 45º. This configuration corresponds to a lift-off case where, according to previous results, shear effects are negligible. In order to compare the results with those obtained by the analytical approach, it is assumed that the span is equal to the length of the specimen, g = 1.

Figure 4 shows the convergence of the displacements on the load application point and on the lift-off corner regarding the number of elements. The displacements obtained in all cases are very similar to the Complete Model of COSMOS/M, but the convergence is faster in the case of IFMD. As the convergence in the mid-point displacement is achieved with 16 elements for IFMD and SM, displacements and stresses will be analyzed for this number of elements. The number of elements along the length and the width of the specimen are specified.

Figure 5 shows the displacements in the middle line and in the load application line corresponding to the IFMD and SM with 16 elements, in comparison with the displacements obtained with the analytical approach. The displacements on the load line determined by IFMD agree better with the analytical and Complete Model results than those obtained by SM.

Figure 6 shows rotations through the length when $y_0 = 0.5$, obtained by SM and IFMD with 16 elements in comparison with the analytical approach. As in the case of the displacements, both θ_x and θ_y rotations obtained by IFMD agree better with the analytical results than SM results with the same number of elements.

Figure 7 shows the distribution through the length of the σ_x and τ_s respectively when $y_0 = 0.5$. In the case of τ_s, the Complete Model predicts a stress concentration effect in the middle point [7], and the analytical results are the average values of the numerical distribution.

Figure 8 shows the distribution through the width of the σ_x and τ_s, when $x_0 = 0.5$. In the load line, σ_x and τ_s obtained analytically are the average values obtained in the Complete Model, and the Complete Model predicts a stress concentration effect. The values of σ_x obtained by IFMD are closer to the analytical approach than those obtained by SM.

Figure 9 shows the distribution through the width of σ_x and τ_s respectively, when $x_0 = 0.25$. Out of the load application point, in the case of σ_x and τ_s the stress distribution in the analytical approach agrees with the average value obtained in the Complete Model. In this case, the results obtained by SM are better than those obtained by IFMD.

According to previous figures, in spite of displacements results are better in the case of IFMD, the same conclusion is not valid in the case of stresses. In order to explain this unexpected result, curvatures are analyzed. Figure 10 shows the curvatures along the length κ_x and κ_s respectively, when $x_0 = 0.5$. With respect to bending curvatures, the agreement with analytic results is very good in both numerical approaches, IFMD and SM. In the case of twisting curvatures κ_s, the agreement with analytic results is better in the case of SM. It seems surprising that after having obtained better displacement and rotations results in the case of IFMD, the curvatures do not follow the same trend. That could be related to the different way in which curvatures are determined in both cases. According to table 1, in SM the curvatures are obtained from Equation (11) after having determined θ_x and θ_y rotations. In the case of IFMD, the curvatures are obtained from Equation (19), after having obtained internal moments without differentiating rotations. As stresses are obtained in both cases from curvatures, this can be the reason of the agreement in stresses obtained by IFMD and SM, shown in Figures 7, 8 and 9.

5. SUMMARY AND CONCLUSIONS

The IFMD has been formulated for a plate element valid for symmetric laminates and it has been compared with SM in the case of a unidirectional off-axis composite in tree-point flexure. Results obtained by both methods with 16 elements are compared with analytical and numerical results that correspond to a fine mesh.

The results in displacements and rotations are better in the case of IFMD than in the case of SM. This is due probably to the fact that IFMD is based on the Principles of Virtual Work and Complementary Virtual Work, whereas SM is based only on the principle of Virtual Work.

Nevertheless, in the case of stresses the results are very similar in both cases. This result is related to the different way of obtaining curvatures in both methods. In SM they are obtained by differentiation of the rotations and in IFMD they are obtained from internal moments. In the present case, the results of curvatures are similar in both cases and consequently, also stress results.

Therefore, the results for a given discretization level are better in IFMD than in SM. In other words, for a given precision of results, the number of elements needed in IFMD is less than in

SM. Then, IFMD appears as an alternative for formulating laminate plate elements, although the diagonalization of the flexibility matrix should be developed for improving its computational cost.

NOMENCLATURE

$\{\varepsilon\}$	Strain vector in the element
$\{\sigma\}$	Stress vector in the element
$\{a^i\}$	Vector of nodal displacements
$\{u\}$	Vector of displacements at any point of the element
$\{\delta a^i\}$	Virtual displacement
$\{P^i\}$	Vector of external forces
$\{F^j\}$	Vector of independent internal forces in the element
$\{\delta F^j\}$	Virtual force
$[K]$	Stiffness Matrix
$[G]$	Flexibility matrix
$[E]$	Equilibrium matrix
$[Y]$	Matrix of forces interpolation functions
$[N]$	Matrix of displacements interpolation functions
$[L]$	Matrix of differential operators
$[B]$	Displacement- strain matrix
$[d]$	Compliance matrix of material
E_L	longitudinal modulus
E_T	transverse modulus
ν_{LT}	in-plane Poisson's ratio
$\nu_{TT'}$	out of plane Poisson's ratio
G_{LT}	in-plane shear modulus
$G_{LT'}$	out of plane shear modulus relating first and third material directions
$G_{TT'}$	out of plane shear modulus relating second and third material directions
θ	Fiber orientation angle
L	span
L'	specimen length
b	specimen width
x_0	x/L
y_0	y/b
c	y/b
g	L/L'
h	specimen thickness
P	load
w_{M1}	displacement at any point in A and D parts
w_{M2}	displacement at any point in B and C parts
w_v	displacement term due to traverse shear in A, B, C, D parts
w_1	total displacement at any point in A and D parts
w_2	total displacement at any point in B and C parts
d_{ij}	in-plane compliance coefficients, where $i,j = x, y, s$
σ_x	in-plane normal stress in the longitudinal direction of the specimen
σ_y	in-plane normal stress in the transverse direction of the specimen
τ_s	in-plane shear stress

REFERENCES

1 Hoa SV, Feng W. Hybrid finite element method for stress analysis of laminate composites. *Kluver academic publishers* 1998.

2 Adarraga I, Cantera A, Romera JM, Insausti N, Mujika F. The dual integrated force method applied to unidirectional composites. *International Journal for numerical methods in engineering* 2014; 98, 9: 663-677.

3. Mujika, F., Berglund, L., Varna, J. and Mondragon, I. 45º Flexure Test for Measurement of In-Plane Shear Modulus. *Journal of Composite Materials* 2002; 36: 2313-2337.

4. Mujika F., Mondragon, I. On the displacement field for unidirectional off-axis composites in 3-point flexure - Part 1: Analytical approach. *Journal of composite materials* 2003; 37: 1041-1066.

5. Mujika, F., de Benito, A. and Mondragon, I. On the Displacement Field for Unidirectional Off-axis Composites in 3-Point Flexure - Part 2: Numerical and experimental results. *Journal of Composite Materials* 2003; 37: 1191-1217.

6. Mujika F. A novel approach for the three-point flexure test of multidirectional laminates. *Journal of Composite Materials* 2012; 46: 259-274.

7. Romera, J.M., Adarraga, I., Cantera, M.A., Mujika F. Numerical analysis of displacement and stress fields of off-axis composites in three-point flexure. *Journal of Composite Materials* 2011; 45: 671-682.

8. Robinson J. (1973). Integrated theory of finite element methods. Wiley and sons.

9. Shames H., Dym C.L. Energy and finite element methods in structural mechanics. Taylor and Francis, 1985. Bristol, Pennsylvania.

10. Patnaik S.N. An integrated method for discrete analysis, *International Journal for Numerical Methods in Engineering*, 1973; 6: 237-251.

11. Patnaik S.N. The integrated force method versus the standard force method. *Comput. Struct* 1986; 22: 151-163.

12. Patnaik S.N, Nagaraj M.S. Analysis of continuum by the integrated force method. *Comput.Struct* 1987; 26: 899-905.

13. Patnaik S.N, Satish H.G. Analysis of continuum using boundary compatibility conditions of integrated force method. *Comput.Struct* 1990; 34 287-295.

14. Patnaik S.N, Berke L, Gallagher R.H. Integrated force method versus displacement method for finite element analysis. *Comput.Struct* 1991; 38: 377-407.

15. Patnaik S.N., Hopkins D.A, Aiello R.A., Berke L. Improved Accuracy for Finite-Element Structural-Analysis via an Integrated Force Method. *Comput.Struct* 1992; 45:521-542.

16. Hopkins D.A., Halford G., Coroneos R., Patnaik S.N. Fidelity of the integrated force method solution. *Int. J. Numer. Methods Eng*. 2002; 55: 1367-1371.

17. Patnaik S.N., Coroneos R., Hopkins D. Significance of strain formulation in theory of solid mechanics 2003; NASA/TM – 212584.

18. Patnaik S.N., Coroneos R, Hopkins D.A.Recent advances in the method of forces: integrated force method of structural analysis, *Adv.Eng.Software* 1998; 29:463-474.

19. Patnaik S.N., Hopkins D.A., Halford G.R. (2004). Integrated Force Method solution to indeterminate structural mechanic problems. NASA/TM – 207430 .

20. Pian HTT. Derivation of element stiffness matrix by assumed stress distribution. MIT 1964, Technical notes.

21. Pian HTT. State of the art development of hybrid/mixed finite element method. *Finite elements in analysis and design* 1995; 21: 5-20.

22. Zhang CH, Feng W, Huang Q. The stress subspace of hybrid stress element and the diagonalization method for flexibility matrix. *Applied mathematics and mechanics* 2002; 23, 11.

23. Zhang CH, Wang D, Zhang J, Feng W, Huang Q. On the equivalence of various hybrid finite elements and a new orthogonatization method for explicit element stiffness formulation. *Finite elements in analysis and design* 2007; 34; 312-332.

24. Dhananjaya H.R., Nagabhushanam J., Pandey P.C. Bilinear plate bending element for thin and moderately thick plates using Integrated Force Method, *Struct. Eng. Mech* 2007; 26: 43-68.
25. Dhananjaya H.R., Nagabhushanam J., Pandey P.C. Automatic generation of equilibrium and flexibility matrices for plate bending elements using Integrated Force Method. *Struct.Eng.Mech* 2008; 30:387-402.
26. Dhananjaya H.R., Pandey P.C., Nagabhushanam J. New eight node serendipity quadrilateral plate bending element for thin and moderately thick plates using Integrated Force Method. *Struct.Eng.Mech* 2009; 33: 485-502.
27. Dhananjaya HR, Nagabhushanam J, Pandey P.C., Jumaat M.Z. New twelve node serendipity quadrilateral plate bending element based on Mindlin-Reissner theory using Integrated Force Method. *Struct.Eng.Mech* 2010; 36: 625-642.
28. Dhananjaya, H. R.; Pandey, P. C.; Nagabhushanam, J.; et al. Closed form solutions for element equilibrium and flexibility matrices of eight node rectangular plate bending element using integrated force method. *Structural Engineering and Mechanics* 2011; 40: 121-148
29. Dhananjaya, H. R.; Pandey, P. C.; Nagabhushanam, J.; et al. New nine-node Lagrangian quadrilateral plate element based on Mindlin-Reissner theory using IFM. *Structural Engineering and Mechanics* 2012; 41: 205-229
30. Fung Y.C. Foundations of solid mechanics. Prentice-Hall International, 1965.
31. Oñate Ibáñez de Navarra E.. Cálculo de estructuras por el método de elementos finitos. Centro Internacional de Métodos Numéricos en Ingeniería, 2nd ed, Cimne, Barcelona, 1995.
32. Rao S. The finite element method in engineering. Elsevier 2005. 4th ed.
33. Hopkins D.A., Patnaik S.N. Stress Formulation in Three-Dimensional Elasticity NASA/TM – 210515, 2001.
34. Kaljevic I., Patnaik S.N., Hopkins D.A. Development of finite elements for two-dimensional structural analysis using the integrated force method, *Comput.Struct* 1996; 59: 691-706.
35. Spilker R.L., Masker S.M., Kania E. Plane isoparametric Hybrid-stress elements: Invariant and optimal sampling. *Int. Journal for numerical methods in engineering* 1981; 17: 1469–1496.
36. Daniel, I.M. and Ishai, O. Engineering Mechanics of Composite Materials. Oxford 2006. University Press, Inc., New York

FIGURE CAPTIONS

Fig. 1 Lift-off at supports in a laminate subjected to three-point flexure.

Fig. 2 Four node rectangular plate element.

Fig. 3 Parts of the specimen defined in the analytical approach.

Fig. 4 Displacements field according to the number of elements. (a) On the load application point. (b) On the Lift-Off point.

Fig. 5 Displacements. (a) In the middle line. $y_0 = 0.5$. (b) In the load line. $x_0 = 0$.

Fig. 6 Rotations in the middle line along the length. (a) θ_x; (b) θ_y.

Fig. 7 Stresses along the length. $y_0 = 0.5$. (a) σ_x; (b) τ_s.

Fig. 8 Stresses along the width. $x_0 = 0.5$. (a) σ_x; (b) τ_s.

Fig. 9 Stresses along the width. $x_0 = 0.25$. (a) σ_x; (b) τ_s.

Fig. 10 Curvatures along the length. $y_0 = 0.5$. (a) κ_x; (b) κ_s.

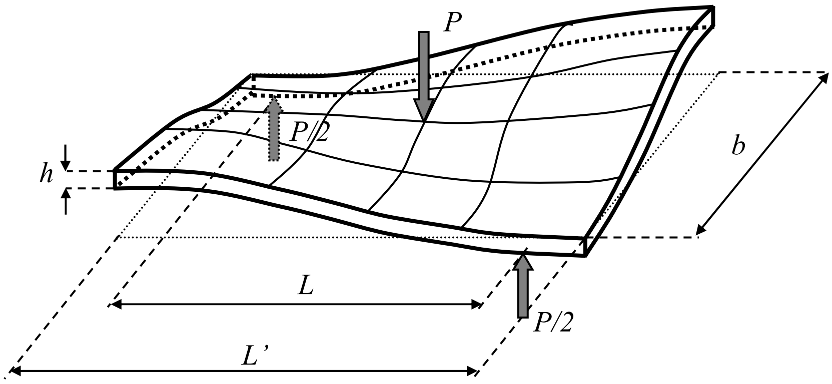

Figure 1. Lift-off at supports in a laminate subjected to three-point bending.

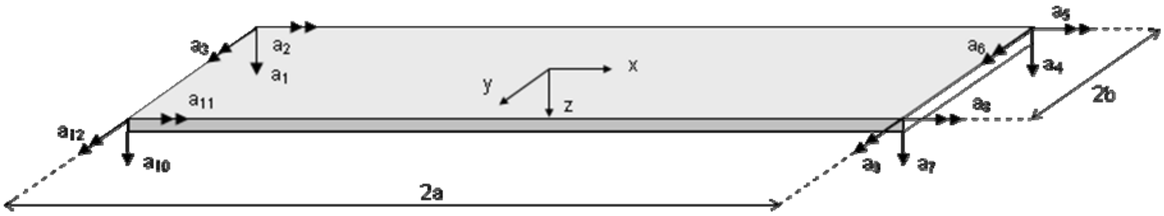

Figure 2. Four node rectangular plate element.

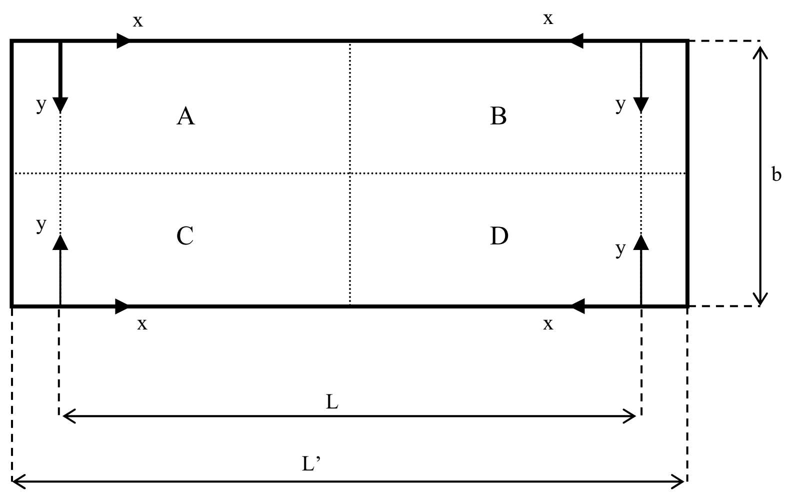

Figure 3. Parts of the specimen defined in the analytical approach.

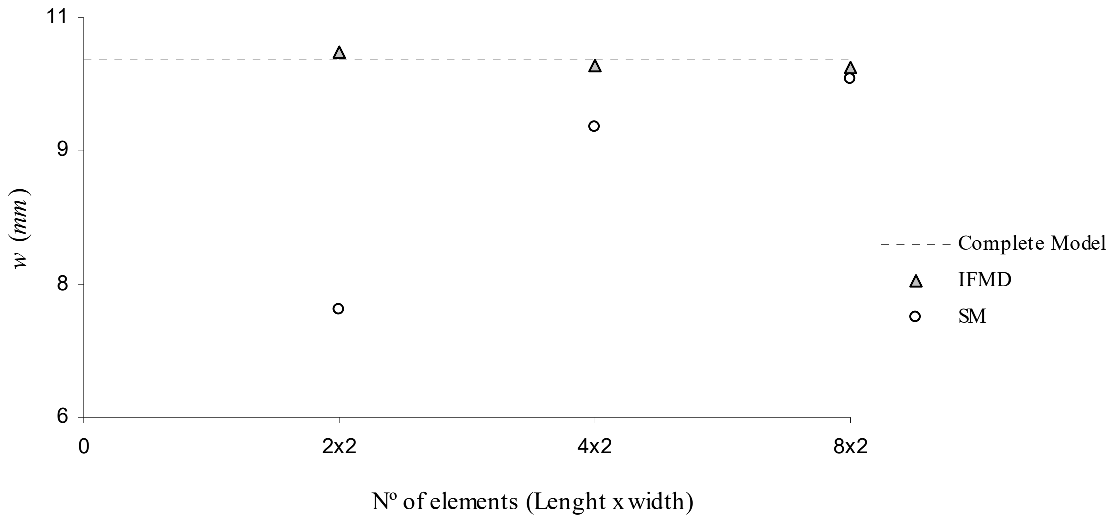

(a)

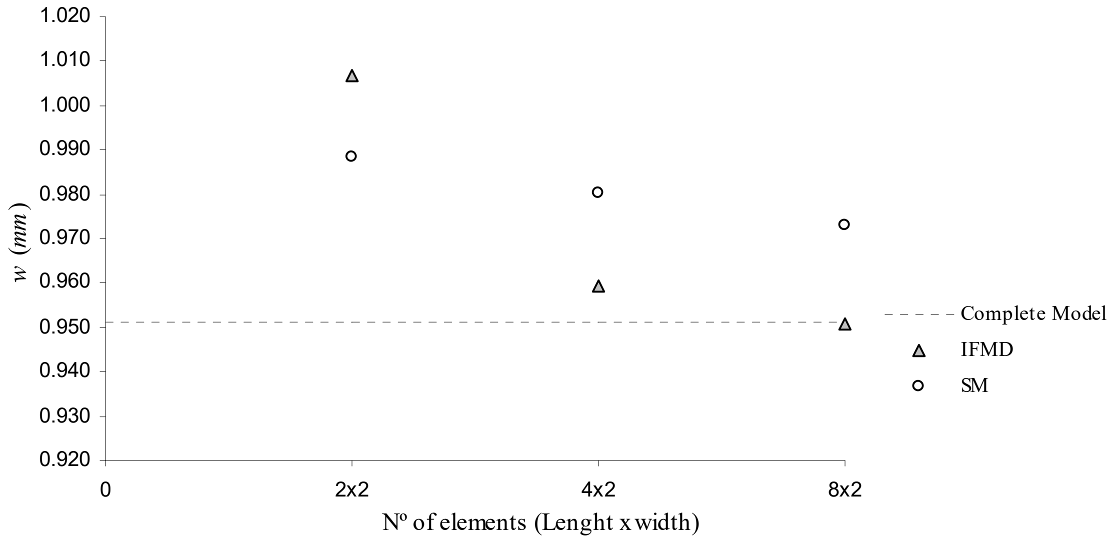

(b)

Figure 4. Displacements field according to the number of elements. (a) Load application point. (b) Lift-Off point.

Fig. 5

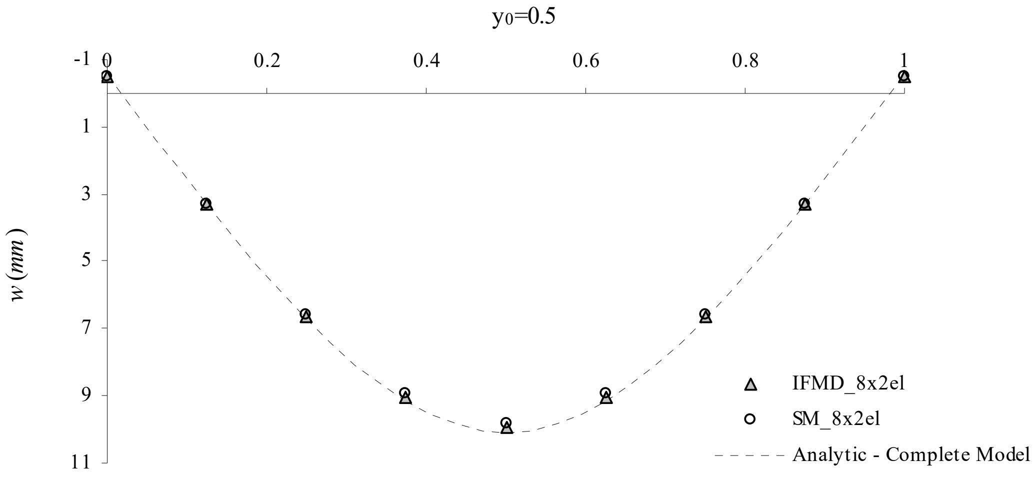

(a)

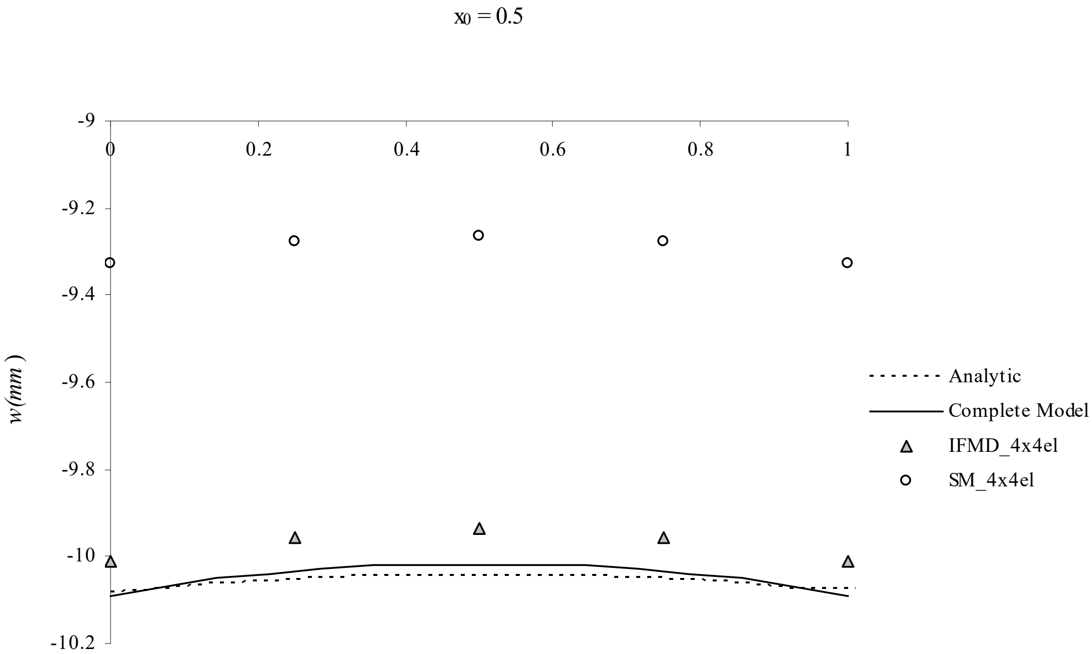

(b)

Figure 5. Displacements. (a) In the middle line. $y_0 = 0.5$. (b) In the load line. $x_0 = 0.5$.

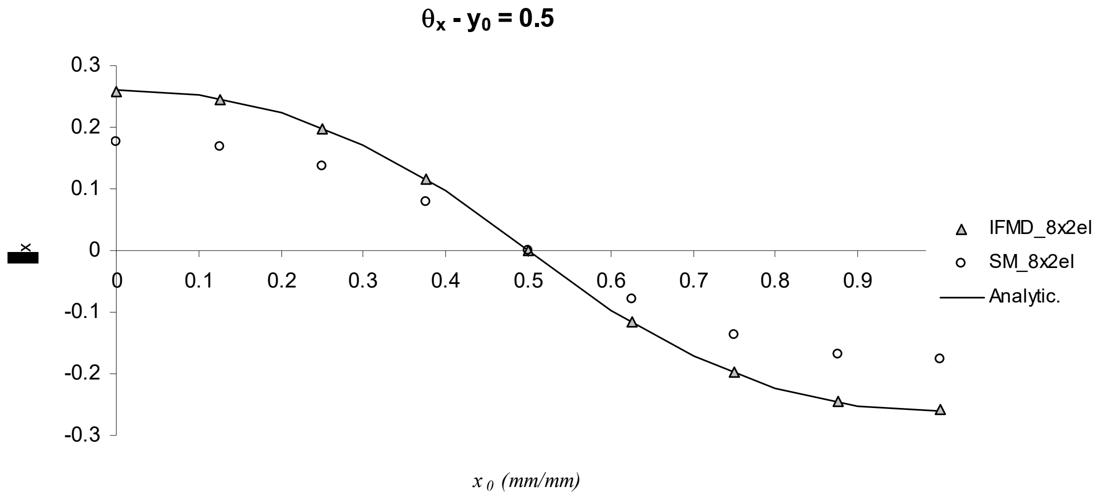

(a)

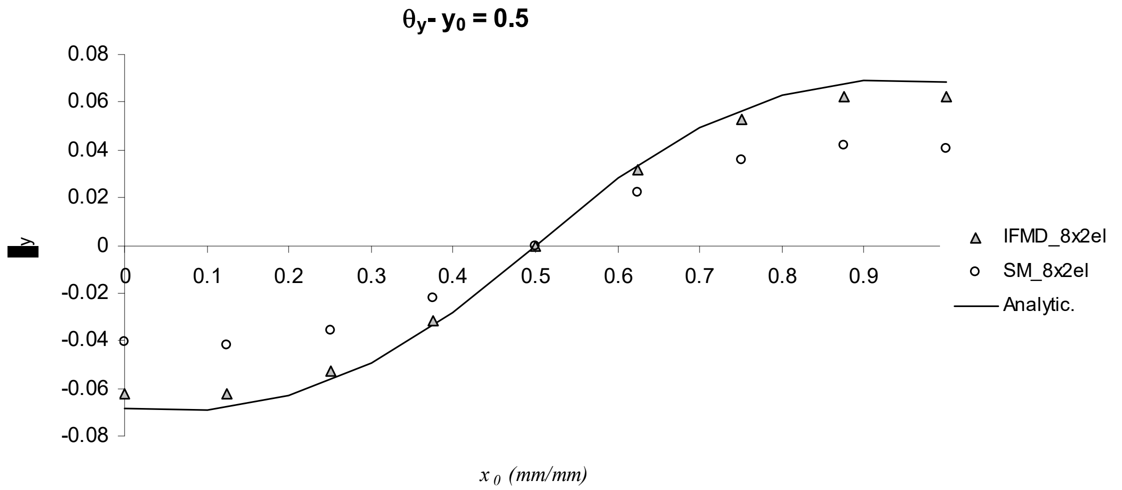

(b)

Figure 6. Rotations in the middle line, $y_0 = 0.5$. (a) θ_x; (b) θ_y.

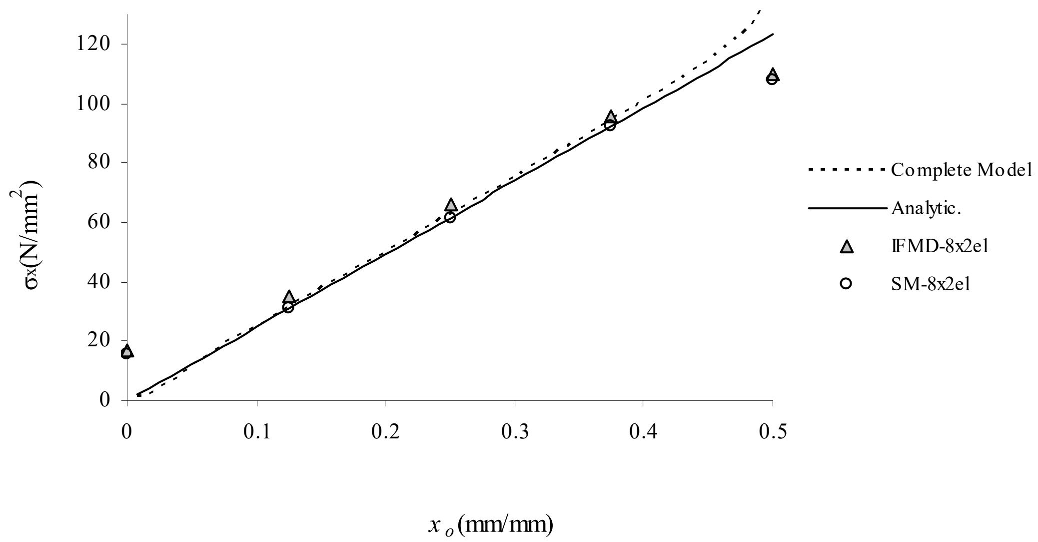

(a)

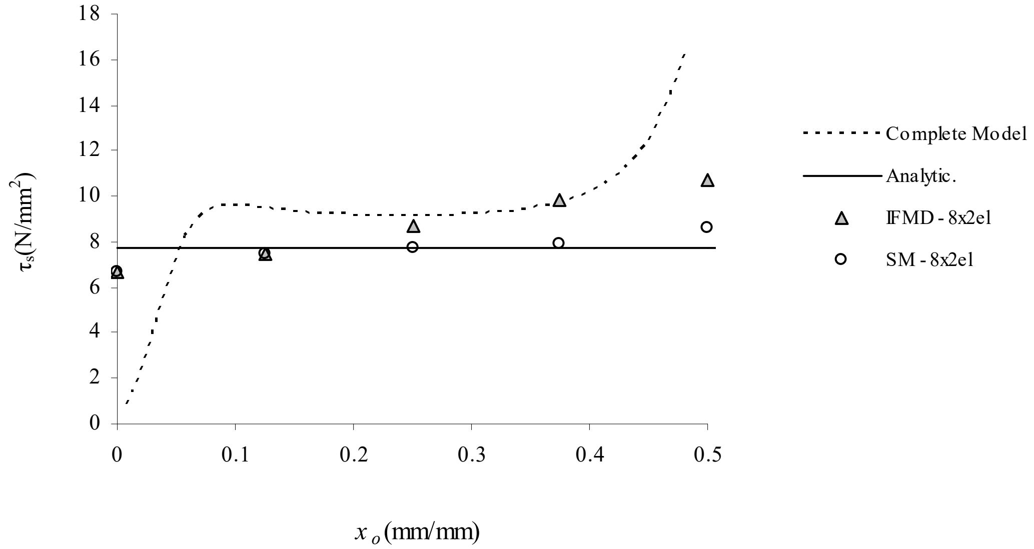

(b)

Figure 7. Stresses along the length, y_0 =0.5. (a) σ_x; (b) τ_s.

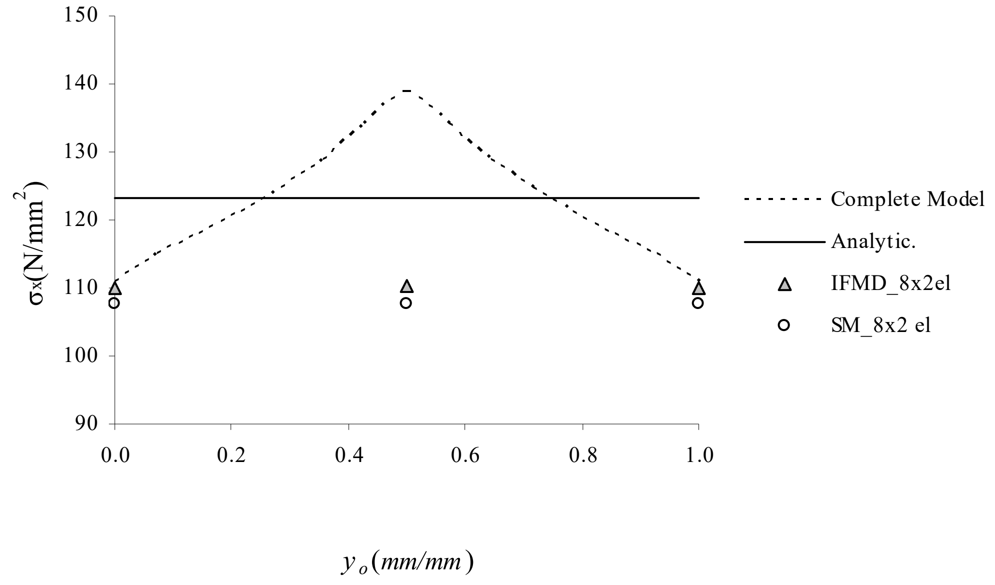

(a)

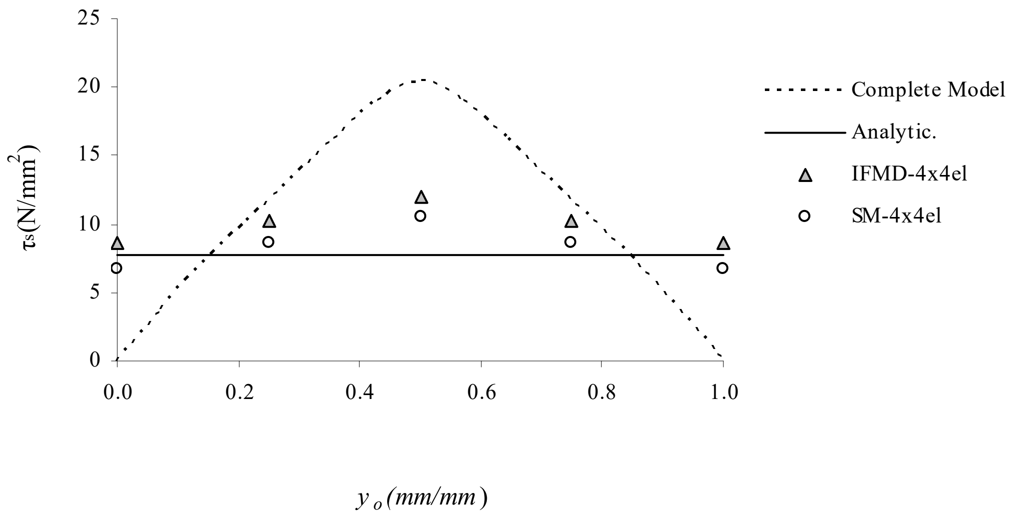

(b)

Figure 8. Stresses along the width on the bottom face, $x_0 = 0.5$. (a) σ_x; (b) τ_s.

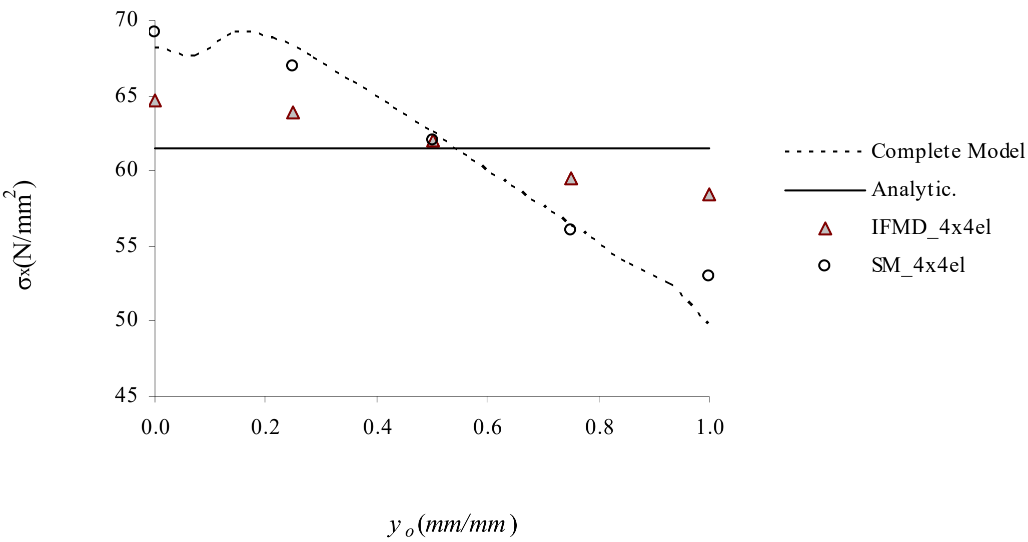

(a)

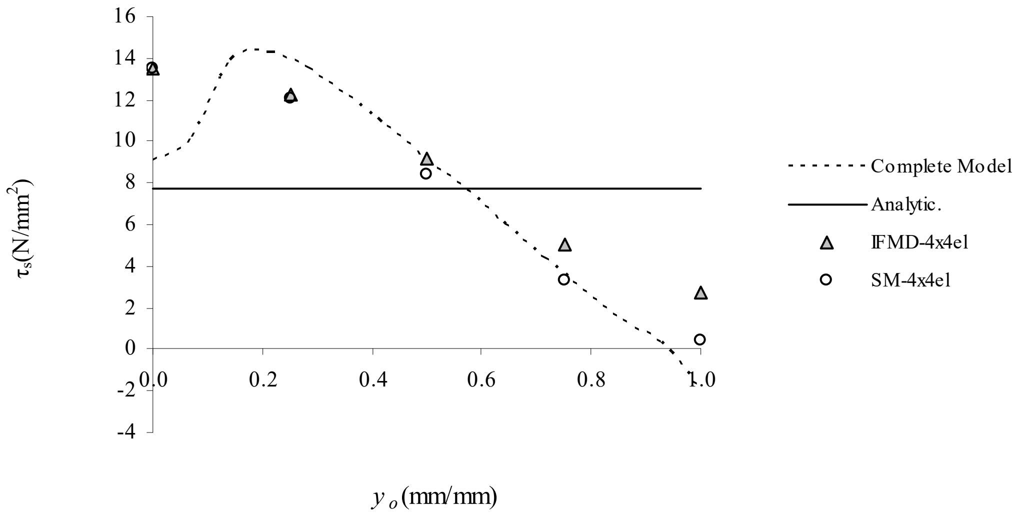

(b)

Figure 9. Stresses along the width on the bottom face, x_0=0.25. (a) σ_x; (b) τ_s.

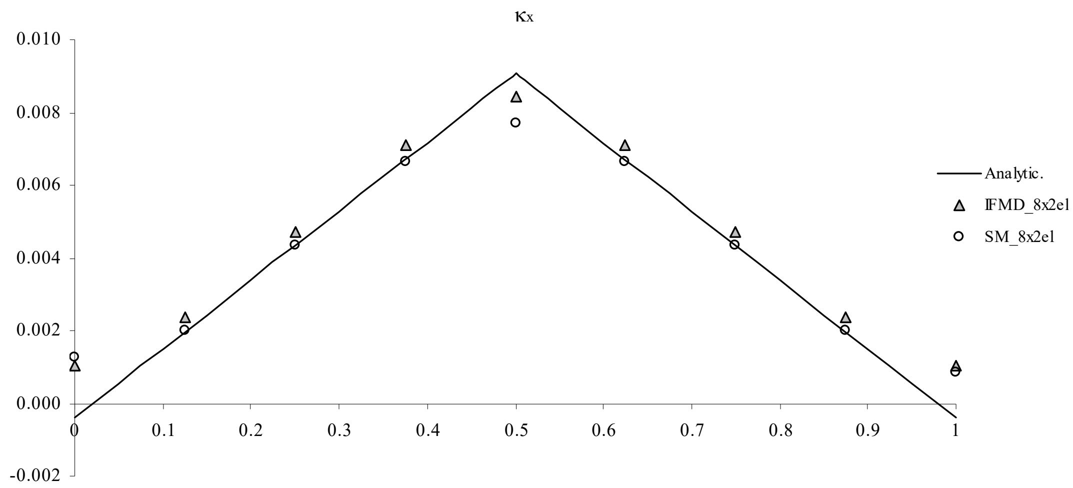

(a)

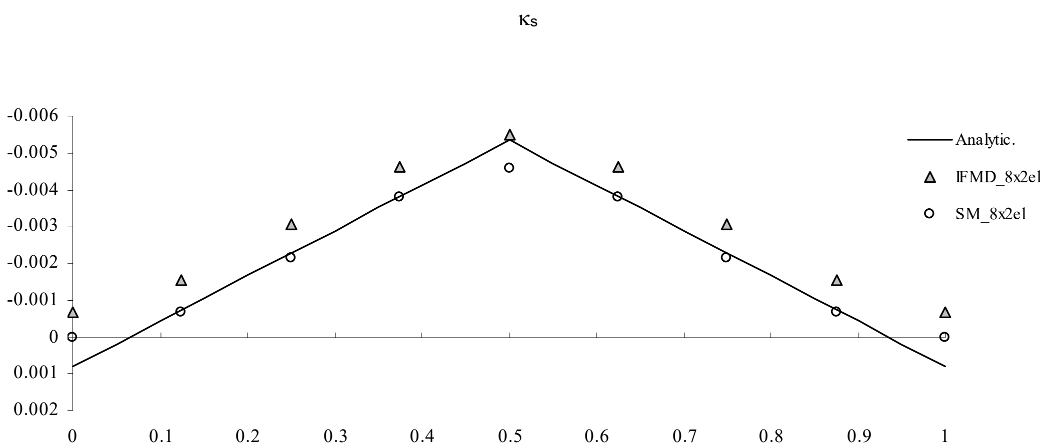

(b)

Figure 10. Curvatures along the length, x_0=0.5. (a) κ_x; (b) κ_s.